Journal of Physics: Conference Series **160** (2009) 012018 doi:10.1088/1742-6596/160/1/012018

Recent results from the DREAM project

Richard Wigmans

Department of Physics
Texas Tech University
Lubbock, TX 79409-1051, U.S.A.

E-mail: wigmans@ttu.edu

Abstract. The aim of the DREAM project is to develop calorimeters that are able to measure the four-vectors of all fundamental constituents of matter, including fragmenting quarks, with a precision of 1% or better. To achieve this, the factors that limit the performance of the present generation of calorimeters are eliminated one by one, in the order at which these factors dominate. In this talk, I give an overview of the results achieved so far, and outline our plans for the future.

1. Introduction

High-precision jet spectroscopy will be increasingly important in future high-energy accelerator experiments, particularly at a Linear e^+e^- Collider. DREAM (Dual REAdout Method) calorimeters seem to be well suited for this task. The key aspect of DREAM detectors is the simultaneous measurement of scintillation light and Čerenkov light generated in the shower development process. By comparing these two signals, the electromagnetic shower fraction can be measured event by event, both for single hadrons and for jets, and the detrimental effects of fluctuations in this fraction can be eliminated.

The merits of this technique were first illustrated with a calorimeter in which the two signals are provided by two different types of optical fibers. More recently, we have been concentrating on crystals ($PbWO_4$ and BGO), which have the potential of eliminating (or at least reducing) the contributions of the next two important sources of fluctuations: photoelectron statistics and sampling fluctuations. I will describe the techniques used to unravel the signals from these crystals into Čerenkov and scintillation components. The detailed time structure measurements we performed for these studies also make it possible to measure the contributions of neutrons to the signals. This would help to reduce the effects of fluctuations in nuclear binding energy losses, which is the last frontier in the quest for ultimate hadronic calorimeter performance. There will be detailed talks about all these aspects at this conference. Gabriella Gaudio will present the evidence for the contribution of Čerenkov light to the signals from $PbWO_4$ crystals, and report on the temperature dependence of this contribution. Cecilia Voena will discuss the precision of event-by-event measurements of the Čerenkov fraction in crystal calorimeters. Davide Pinci will show results of dual-readout calorimetry performed with simple crystal electromagnetic calorimeters used in conjunction with our DREAM fiber module, and John Hauptman will talk about the neutron contributions to the signals. Finally, Roberto Carosi will describe a new system intended to measure the time structure of all our signals with nanosecond resolution. In this talk, I will provide context and mention some highlights.

2. Dual-Readout Calorimetry

The DREAM Collaboration tries to improve the performance of hadron calorimeters by eliminating or reducing the factors that limit that performance. Since the resolution of calorimeters is determined by fluctuations, eliminating or reducing the (effects of the) dominant fluctuations is the key to improving it. In non-compensating calorimeters, the hadronic energy resolution is dominated by fluctuations in the em shower fraction, $f_{\rm em}$. DREAM has shown that (the effects of) these fluctuations can be eliminated by simultaneously measuring both the visible deposited energy (dE/dx) and the Čerenkov light generated in the shower absorption process.

Calorimeters that use Čerenkov light as signal source are, for all practical purposes, only responding to the em fraction of hadronic showers [1]. This is because the electrons/positrons through which the energy is deposited in the em shower component are relativistic down to energies of only 200 keV. On the other hand, most of the non-em energy in hadron showers is deposited by non-relativistic protons generated in nuclear reactions [2]. Such protons do generate signals in other types of active media (scintillator, LAr). By comparing the relative strengths of the two signals, the em shower fraction can be determined and the total shower energy can be reconstructed using the known e/h value(s) of the calorimeter. This can be seen as follows. The measured calorimeter signal can be written as the sum of an em term and a non-em term. The latter is affected by the e/h ratio:

$$\begin{aligned} S &= E\left[f_{\rm em} + (h/e)_S(1-f_{\rm em})\right] \\ Q &= E\left[f_{\rm em} + (h/e)_Q(1-f_{\rm em})\right] \end{aligned} \tag{1}$$

The scintillator (S) and Čerenkov (Q) signals are different because of differences in the e/h ratios. When these e/h ratios are known, these equations can either be solved for the em shower fraction ($f_{\rm em}$) or for the shower energy (E).

2.1. Fiber-based detectors

This principle was first demonstrated with a calorimeter that used two active media, hence the name DREAM (Dual REAdout Method): scintillating fibers measured the visible shower energy (S), while clear fibers measured the generated Čerenkov light (Q). Using the ratio of the two signals, the value of $f_{\rm em}$ could be determined *event-by-event*, since

$$\frac{Q}{S} = \frac{f_{\rm em} + 0.21\,(1-f_{\rm em})}{f_{\rm em} + 0.77\,(1-f_{\rm em})} \tag{2}$$

where 0.21 and 0.77 represent the h/e ratios of the Čerenkov and scintillator calorimeter structures, respectively.

The merits of this method are clearly illustrated by Figure 1, which shows the overall Čerenkov signal distribution for 100 GeV π^- (a), as well as distributions for subsamples selected on the basis of their $f_{\rm em}$ value (b) [3], determined by Equation 2. Each $f_{\rm em}$ bin probes a certain region of the overall signal distribution, and the average value of the subsample distribution increases with $f_{\rm em}$.

Once the value of $f_{\rm em}$ was determined, the signals could be corrected in a straightforward way for the effects of non-compensation. In this process, the energy resolution improved, the signal distribution became much more Gaussian and, most importantly, the hadronic energy was correctly reproduced. This was true both for single pions as well as for jets The results for 200 GeV "jets" are shown in Figure 1c-e. These "jets" were in fact not fragmenting quarks or gluons, but multiparticle events created by pions interacting in a target placed upstream of the calorimeter. Using only the *ratio* of the two signals produced by this calorimeter, the resolution for these "jets" was improved from 14% to 5%, in the Čerenkov channel. It was shown that this 5% resolution was in fact dominated by fluctuations in side leakage in this (small, only 1030 kg instrumented volume) detector. Eliminating such fluctuations led to a further considerable improvement (Figure 1e).

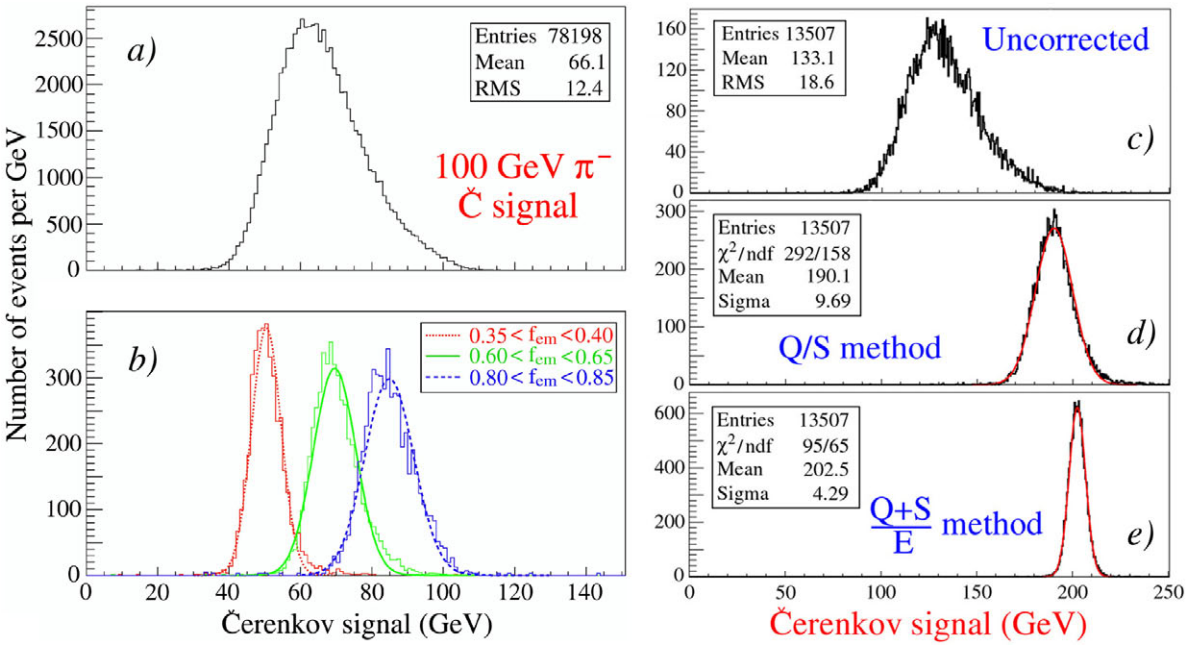

Figure 1. Čerenkov signal distribution for 100 GeV π^- (a) and distributions for subsamples of events selected on the basis of the measured $f_{\rm em}$ value, using the Q/S method (b). Signal distributions for high-multiplicity 200 GeV "jets" in the DREAM before (c) and after (d) corrections on the basis of the observed Čerenkov/scintillator signal ratio were applied. In diagram e, energy constraints were used, which eliminated the effects of lateral shower fluctuations that dominate the resolution in d [3].

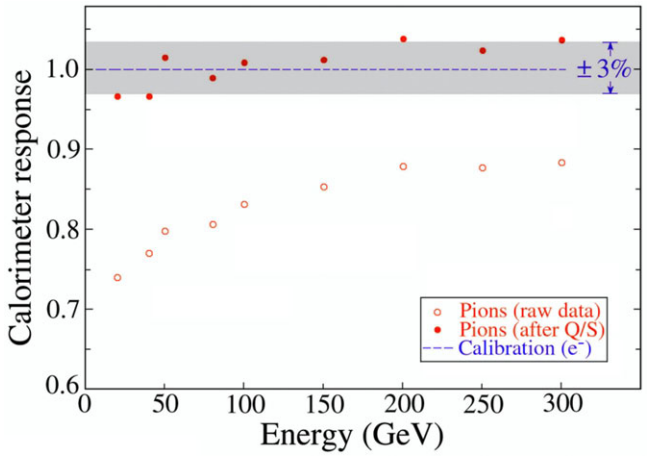

Figure 2. The calorimeter response (average signal per unit energy) for pions before and after the corrections based on a comparison of the scintillator and Čerenkov signals were applied [3].

The shower energy could also be determined directly (*i.e.,* without first measuring $f_{\rm em}$) by solving Equations 1 for E:

$$E = \frac{S - \chi C}{1 - \chi}, \quad \text{with } \chi = \frac{1 - (h/e)_S}{1 - (h/e)_C} \sim 0.3 \text{ for this calorimeter} \tag{3}$$

Figure 2 illustrates that the hadronic signal non-linearity (a notorious problem for non-compensating calorimeters) was indeed more or less eliminated with such a procedure, and that the calorimeter response to pions became within a few percent equal to that for electrons, with which the instrument

was calibrated. Also the "jet" energy was well reconstructed in this way. Whereas the raw data gave a mean value of 133.1 GeV for 200 GeV "jets" (Figure 1c), the described procedure increased it to 190.1 GeV (Figure 1d). Any remaining discrepancies are most likely due to the effects of side leakage, and could thus be eliminated in a sufficiently large detector.

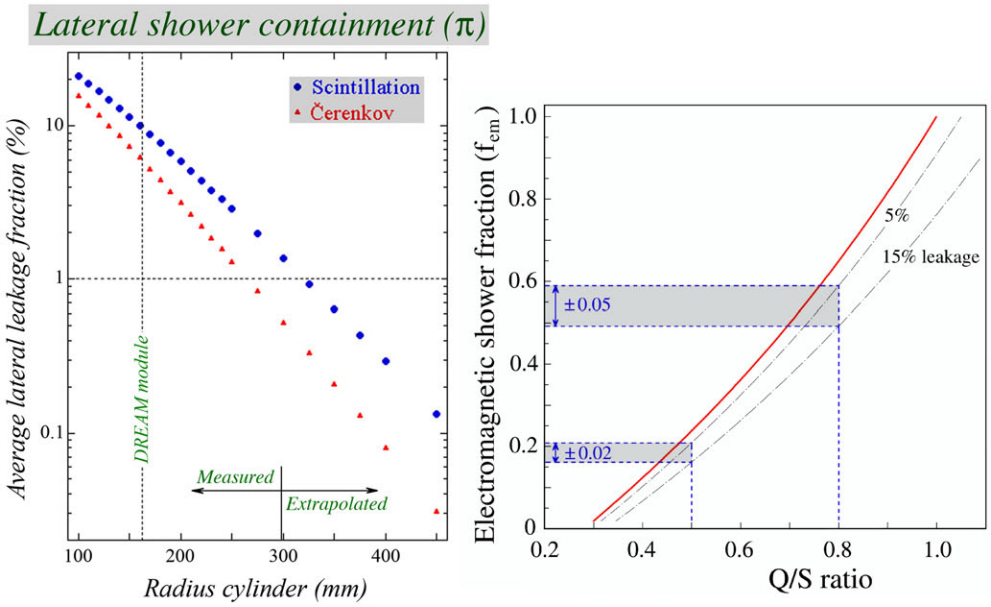

Figure 3. Leakage outside of a DREAM calorimeter cylinder, as a function of the radius of that cylinder. Results are given for 100 GeV π^+ as a fraction of the total signal in an infinitely large calorimeter, separately for scintillation and Čerenkov light (a). The relationship between the em shower fraction needed for the correction procedures and the measured Q/S signal ratio. This relationship is given for a perfect calorimeter and for calorimeters that are too small to fully contain the hadron showers (b) [4].

The importance of shower leakage in this relatively small calorimeter is illustrated in Figure 3. Figure 3a shows that for showers induced by 100 GeV pions, on average $\sim 90\%$ of the scintillator signal and $\sim 95\%$ of the Čerenkov signal that would be recorded in an infinitely large instrument of this type is observed in our detector. The effects of this leakage on the calorimeter performance are illustrated in Figure 3b, which shows the relationship between the em shower fraction ($f_{\rm em}$) which one needs to know for the correction procedure, and the Q/S signal ratio which is measured. Event-to-event fluctuations in shower leakage lead to an uncertainty in the value of $f_{\rm em}$ derived from these measurements, and this uncertainty affects the energy resolution and the value of the reconstructed energy. Figure 3a also shows that in order to reduce the average energy leakage fraction from 10% to 1%, the radius of the detector would have to be roughly doubled.

2.2. Homogeneous DREAM calorimeters

Once the effects of the dominant source of fluctuations are eliminated, the resolution is determined and limited by other types of fluctuations. In the case of the DREAM detector, these fluctuations include, apart from fluctuations in side leakage which can be eliminated by making the detector sufficiently large (see Figure 1e), *sampling fluctuations* and fluctuations in the *Čerenkov light yield*. The latter effect alone (8 Čerenkov photoelectrons per GeV) contributed $35\%/\sqrt{E}$ to the measured resolution. Both effects could be greatly reduced by using crystals for dual-readout purposes. Certain dense high-Z crystals ($PbWO_4$, BGO) produce significant amounts of Čerenkov light, which may be separated from the scintillation light by exploiting differences in time structure, spectral properties and directionality.

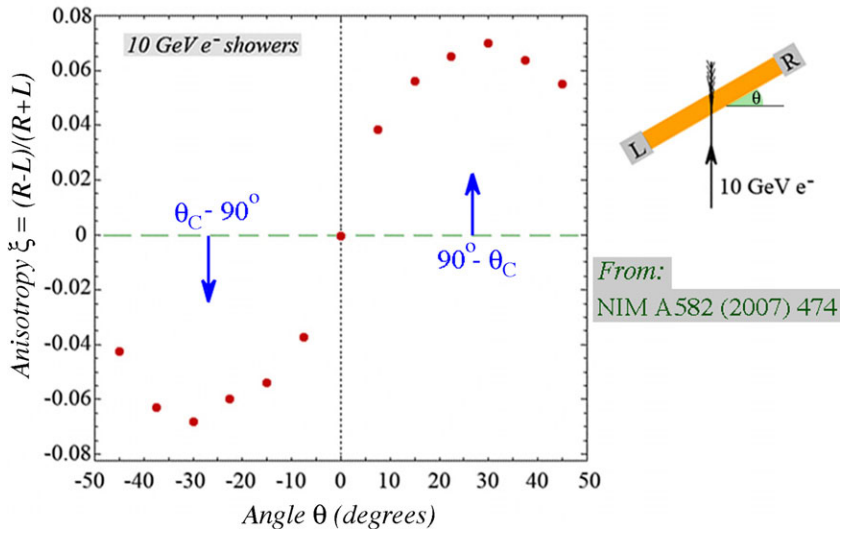

Figure 4. Left-right response asymmetry measured for 10 GeV electrons showering in a $2.5X_0$ thick $PbWO_4$ crystal, as a function of the orientation of the crystal (the angle θ) [5].

Figure 4 provides proof that a significant fraction of the response from a scintillating $PbWO_4$ crystal is indeed due to Čerenkov light. The figure shows an angle-dependent asymmetry between the signals from the two PMTs (L and R) located at opposite ends of a crystal exposed to a beam of 10 GeV electrons. This asymmetry indicates the presence of a directional component in the light produced in this crystal. This component is largest when the crystal is oriented at such an angle that the Čerenkov light emitted by the particles strikes the PMT that records it perpendicularly, *i.e.*, at $\theta \sim 27^\circ$ for PMT R and at $\theta \sim -27^\circ$ for PMT L (the Čerenkov angle in $PbWO_4$ is 63°) [5].

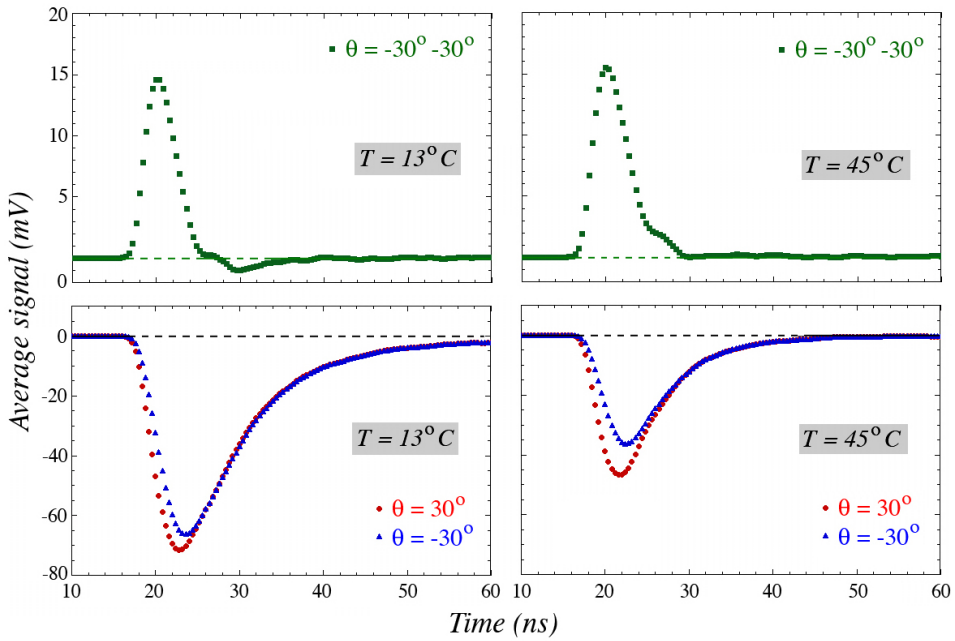

Figure 5. Average time structure of the signals from PMT R (see Figure 4) measured for 50 GeV electrons traversing the $PbWO_4$ crystal at $\theta = 30^\circ$ and $\theta = -30^\circ$ (*bottom* plots), as well as the difference between these two signals (*top* plots), measured for two different temperatures: 13°C (*left*) and 45°C (*right*) [6].

Figure 5 shows the time structure of the signals from a lead tungstate crystal traversed by a beam of 50 GeV electrons, for two different angles and two different temperatures. Each of the bottom graphs depicts the average time structures of the signals measured at $\theta = 30^\circ$ and $\theta = -30^\circ$ with PMT R. The difference between the signals recorded at these two angles is shown in the top graphs, separately for each of the two temperatures. At $\theta = 30^\circ$, Čerenkov light produced in the showers initiated in the crystals by the high-energy electrons is preferentially detected in PMT R, since this light is emitted at an angle of $\arccos(1/n) = 63^\circ$ by the charged relativistic shower particles traversing the $PbWO_4$ crystal (which has a refractive index $n = 2.2$). This Čerenkov light manifests itself as an additional prompt component, superimposed on the scintillation light that constitutes practically the entire signal measured at $\theta = -30^\circ$. As a result, the signals measured at $\theta = 30^\circ$ are larger, and rise steeper than those measured with the same PMT at $\theta = -30^\circ$. For PMT L, the opposite effect was observed. As expected, here the signals at $\theta = -30^\circ$ were measured to be larger and steeper than those at $\theta = 30^\circ$.

Interestingly, the Čerenkov component was not affected by the change in temperature. However, the intensity of the scintillation component decreased by about a factor of two when the temperature was increased from 13 to 45°C. As a result, the contribution of Čerenkov light is much more evident from the time structure measured at the higher temperature [6].

Details of the time structure of the $PbWO_4$ signals have been successfully used to measure the Čerenkov/scintillation ratio for individual events [7], and the em fraction of hadron-induced showers in a calorimeter system with a $PbWO_4$ em section [8, 9].

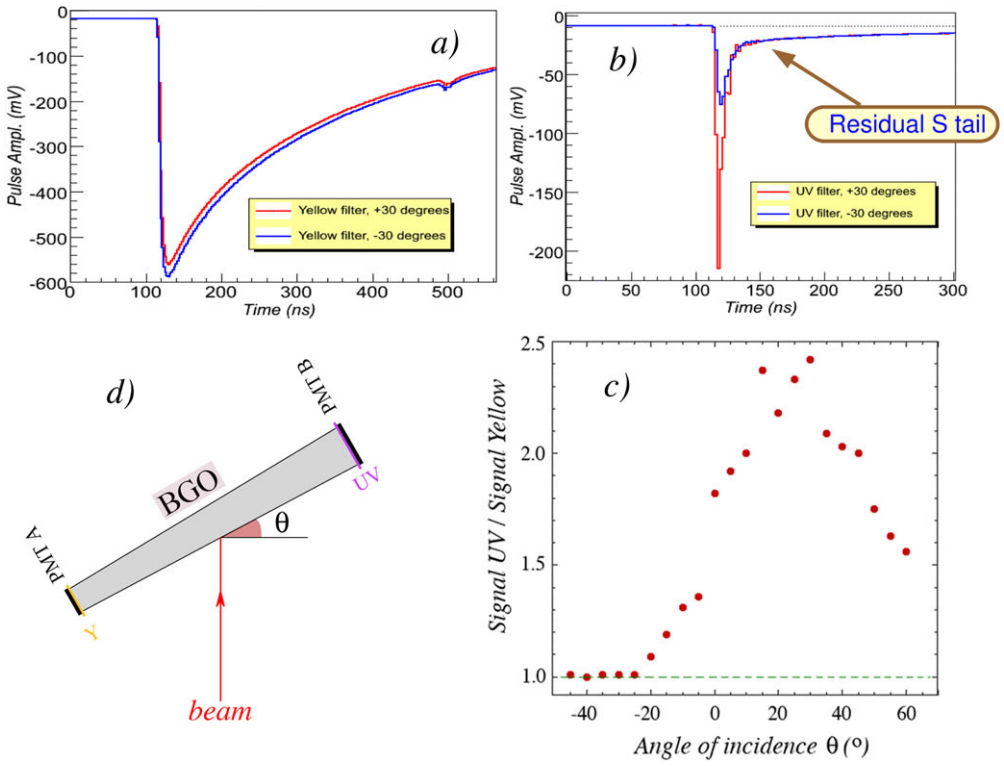

Figure 6. Average signals produced by 50 GeV electrons traversing a BGO crystal at angles of $\pm 30^\circ$ with the longitudinal axis (d), as measured with a UV filter (b), or with a yellow filter (a). The ratio of these two signals, as a function of the angle of incidence of the beam electrons (c) [7].

Even more interesting features were observed in bismuth germanate ($Bi_4Ge_3O_{12}$, or BGO) crystals. Even though Čerenkov radiation represents a much smaller fraction of the light produced by these crystals, it is easier to separate and extract it from the signals. The much longer scintillation time constant and the spectral difference are responsible for that. Figure 6 shows recent results obtained

by the DREAM Collaboration. The different spectra for the scintillation and Čerenkov light are evident from Figures 6a and b, which show the time structures of signals recorded with two different filters. The "prompt" component observed in the ultraviolet signal is due to Čerenkov light. This can be concluded from Figure 6c, which shows the ratio of both signals as a function of the angle of incidence of the beam electrons. This ratio peaks when the photons emitted at the Čerenkov angle ($\theta_C = \arccos 1/n \approx 63°$) travel along the longitudinal crystal axis: $\theta = 27°$ (Figure 6d).

Figure 6b shows that also a small fraction of the scintillation light passes through the UV filter. This offers the possibility to obtain all needed information from that one signal. An external trigger opens two gates: one narrow (10 ns) gate covers the prompt component, the second gate (delayed by 30 ns and 50 ns wide) only contains scintillation light. The latter signal can also be used to determine the contribution of scintillation to the light collected in the narrow gate. In this way, the Čerenkov/scintillation ratio can be measured event-by-event on the basis of one signal only [7]. We have used this technique to assess the possibilities for dual-readout calorimetry with a crystal em calorimeter section [9].

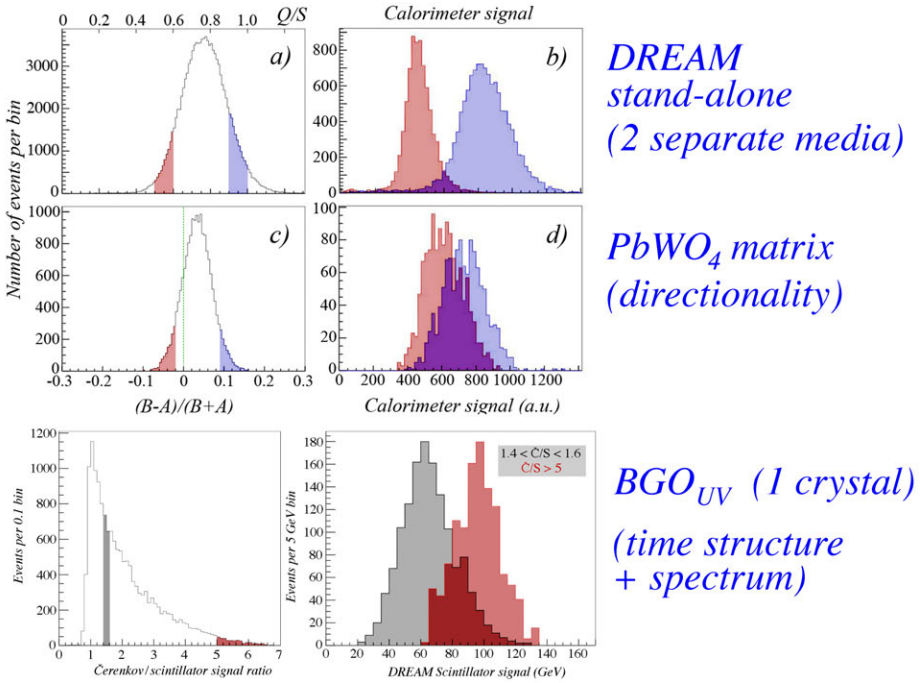

Figure 7. Total hadronic signal distribution in the DREAM fiber calorimeter, for two event samples with a different electromagnetic fraction (b, d, f). The em fraction was determined on the basis of the Q/S signal ratio in the fiber calorimeter itself (a) [5], from the directionality of the signals measured in a $PbWO_4$ crystal matrix installed upstream (c) [8]), or from the time structure of the signals from an upstream BGO crystal (e) [9].

In Figure 1, we showed how the measurement of the em shower fraction, $f_{\rm em}$, (from the Čerenkov/scintillation ratio) for individual events was crucial for improving the hadronic calorimeter performance: event samples with different $f_{\rm em}$ values represented different regions of the total signal distribution. As illustrated in Figure 7, we have observed similar effects for calorimeters in which one or more crystals served as an em section. Figure 7c,d shows results of tests in which the fiber calorimeter was used in conjunction with a matrix of 19 $PbWO_4$ crystals which served as an em calorimeter section, read out by two PMTs. The asymmetry in the signals from these two PMTs was used as a measure of the em content of the developing shower. Figure 7d shows that the total signal in the combined calorimeter system depended indeed in the expected way on this measured asymmetry [8]. Figure 7e,f concerns the results of similar tests with a BGO crystal serving as the em calorimeter section. In this case, the em shower fraction was derived from the time structure of the signals from this crystal (see also Figure 6b).

Figure 7f shows that the total calorimeter signal is indeed very sensitive to the em fraction measured in this way: a large em fraction leads to a large total signal, a small em fraction to a small total signal, just as in the measurements of the fiber calorimeter in stand-alone mode, which are shown for reference purposes in Figure 7a,b [9]. In these measurements, the Čerenkov signals from the crystals were found to comprise a substantially larger number of photoelectrons than those from the quartz fibers: > 30 photoelectrons/GeV.

2.3. Further improvements

The features described above offer the potential to improve the already impressive DREAM results significantly. Should one succeed to eliminate, or at least greatly reduce the contributions of sampling fluctuations and photoelectron statistics to the hadronic energy resolution in this way, then the last hurdle toward ultimate performance is formed by the fluctuations in visible energy, *i.e.,* fluctuations in the energy fraction used to break up atomic nuclei. It has been demonstrated that the kinetic energy carried by the neutrons produced in the shower development process is correlated to this invisible energy loss [2]. Efficient neutron detection, a key ingredient for compensating calorimeters, not only brings e/h to 1.0, but also greatly reduces the contribution of fluctuations in invisible energy to the hadronic energy resolution. It has been demonstrated that this reduces the ultimate limit on this resolution to $\sim 13\%/\sqrt{E}$ [10], in compensating lead/plastic-scintillator calorimeters. This would translate into mass resolutions of $\sim 1.5\%$ for hadronically decaying W and Z bosons, much better than the requirements of a Linear e^+e^- Collider experiment.

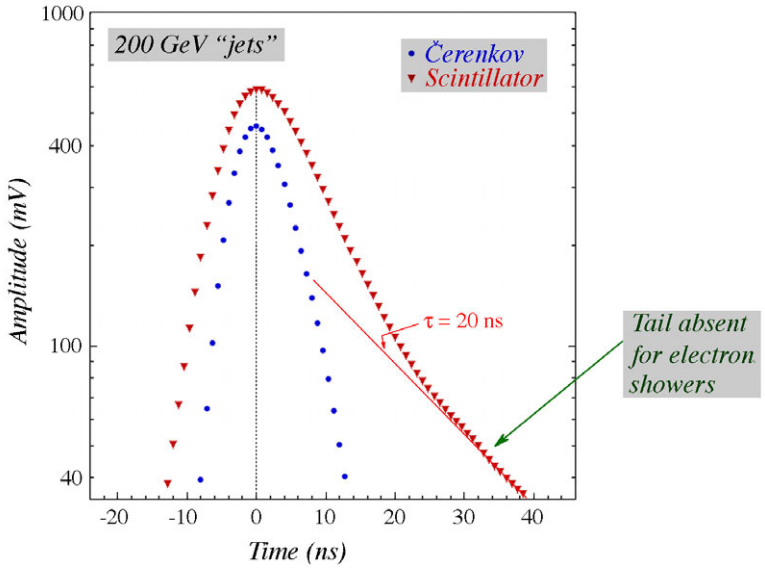

Figure 8. Average time structure of the Čerenkov and scintillation signals recorded for 200 GeV "jets" developing in the DREAM calorimeter. The scintillation signals exhibit a tail with a time constant of about 20 ns, which is absent in the Čerenkov signals. [11].

Detailed measurements of the time structure of the calorimeter signals, examples of which are given in Figures 5 and 6, make it also possible to measure the contribution of neutrons to the shower signals. Figure 8 illustrates this with data recently taken with the DREAM fiber calorimeter [11]. The figure shows the average time structure of Čerenkov and scintillator signals measured for 100 GeV π^+ showers developing in this calorimeter. The scintillator signals exhibit an exponential tail with a time constant of ~ 20 ns. As we established earlier [12], this tail has all the characteristics expected of a (nonrelativistic) neutron signal and is thus absent in the time structure of the Čerenkov signals.

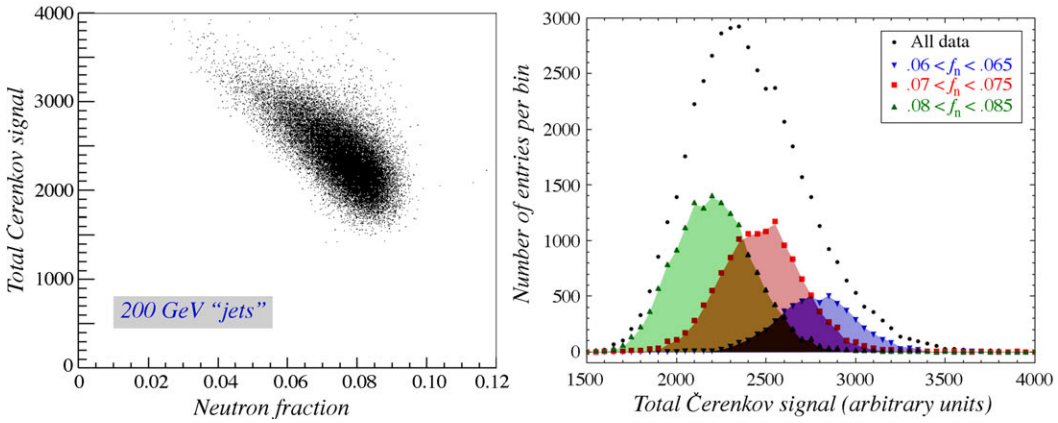

Figure 9. Scatter plot for 200 GeV "jets. For each event, the combination of the total Čerenkov signal and the fractional contribution of neutrons to the total scintillator signal is represented by a dot (left diagram). Distribution of the total Čerenkov signal for 200 GeV "jets" and the distributions for three subsets of events selected on the basis of the fractional contribution of neutrons to the scintillator signal (right) [11].

The new data (obtained for the entire detector, instead of individual towers) made it possible to measure the relative contribution of neutrons to the scintillator signals, f_n, event-by-event. Figure 9 shows that this neutron fraction is clearly anti-correlated to the total Čerenkov signal (left diagram), and that a subsample of events with (approximately) the same f_n value corresponds to a certain region of the total signal distribution (right diagram), in much the same way as the $f_{\rm em}$ fraction probes the total signal distribution (Figure 1b). And just as for the $f_{\rm em}$ measurements, this information could be used to

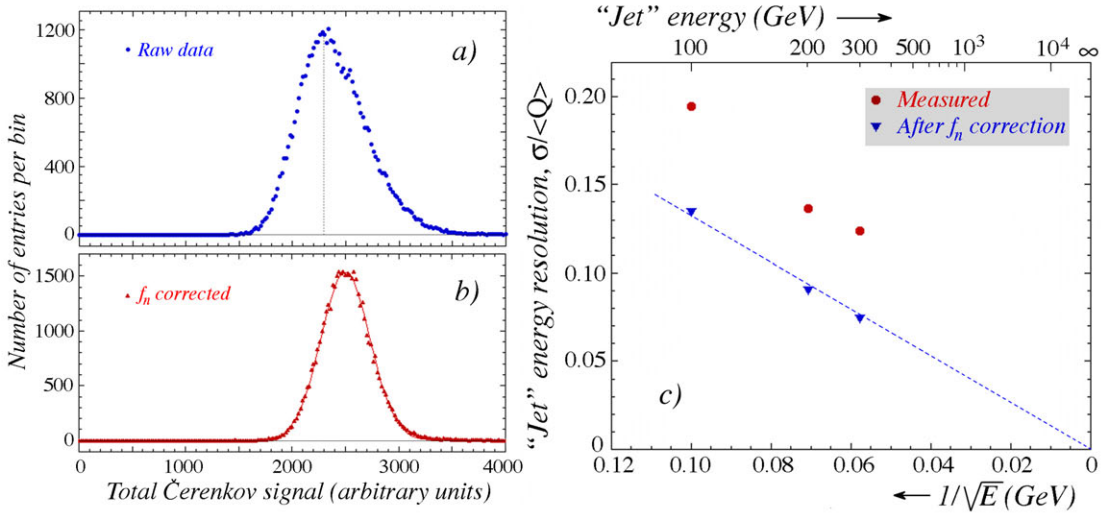

Figure 10. Distribution of the total Čerenkov signal for 200 GeV "jets" before (a) and after (b) applying the correction based on the measured value of f_n, described in the text. Relative width of the Čerenkov signal distribution for "jets" as a function of energy, before and after a correction that was applied on the basis of the relative contribution of neutrons to the scintillator signals (c) [11].

improve the hadronic performance of the fiber calorimeter. This is illustrated in Figure 10, which shows that the asymmetric signal distribution characteristic for a non-compensating calorimeter (Figure 10a) could be transformed into a narrower, Gaussian distribution (Figure 10b), and that in this process any non-Poissonian contributions to the energy resolution were eliminated (Figure 10c).

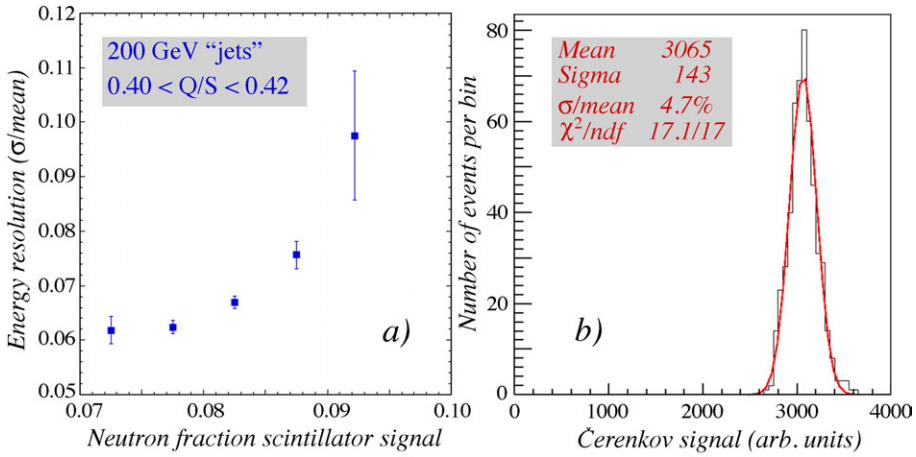

Figure 11. The energy resolution for 200 GeV "jets" with the same em shower fraction, as a function of the fractional neutron contribution to the scintillator signals (a). Čerenkov signal distribution for 200 GeV "jets" with $0.70 < Q/S < 0.75$ and $0.45 < f_n < 0.65$, together with the results of a Gaussian fit (b) [11].

We would like to point out that these improvements were achieved by using the information from only *one* type of fiber, *i.e.,* the time structure of the signals from the scintillating fibers. This in contrast to the improvements resulting from the measurements of $f_{\rm em}$, which require two different types of fiber. However, the (anti-)correlation between f_n and $f_{\rm em}$ is not perfect. The elimination of fluctuations in $f_{\rm em}$ takes care of the effects of the *average* contribution of invisible energy. However, for a given value of $f_{\rm em}$, the invisible energy fluctuates about this average, and a measurement of f_n may track these fluctuations. Therefore, measurements of f_n provide information *complementary* to that obtained from the Q/S signal ratio.

This is illustrated in Figure 11a, which shows that the energy resolution of a subsample of 200 GeV "jet" events with (approximately) the same em shower fraction is clearly affected by the relative contribution of neutrons to the signals. As f_n increases, so does the fractional width of the Čerenkov signal distribution. A larger $f_n$values means that the average invisible energy fraction is larger. This in turn implies that the event-to-event fluctuations in the invisible energy are larger, which translates into a worse energy resolution, even in signals to which the neutrons themselves do not contribute. Figure 11b illustrates the quality of the response function that was achieved with the combined information on the em shower fraction and the contribution of neutrons to the signals. This Čerenkov signal distribution concerns 200 GeV "jet" events with a Q/S value between 0.70 and 0.75 and a fractional neutron contribution to the scintillator signals between 0.045 and 0.065. The distribution is very well described by a Gaussian fit, with an energy resolution of 4.7%. The resolution was further reduced, to 4.4%, when the neutron fraction was narrowed down to 0.05 - 0.055. As a reminder, we mention that these results were achieved in a calorimeter with an instrumented mass of only about 1 ton. The mentioned resolutions are most likely strongly dominated by the contributions of (Čerenkov) photoelectron statistics (estimated at 2.5%) and side leakage. Eliminating these remaining factors, by means of more efficient detection of the Čerenkov signal in a sufficiently large detector may bring the resolution close to the theoretical limits.

3. Future plans

High-quality energy measurements will be an important tool for accelerator-based experiments at the TeV scale. There are no fundamental reasons why the four-vectors of all elementary particles could not be measured with a precision of 1% or better at these energies. However, reaching this goal is far from trivial, especially for the hadronic constituents of matter. Unfortunately, little or no guidance is provided

by hadronic Monte Carlo shower simulations in this respect. In the past 30 years, all progress in this domain therefore has been achieved through dedicated R&D projects such as DREAM, and this is still the way to go today.

The dual-readout R&D project concentrates strongly on experimental tests of the validity of the principles on which improvement of hadronic calorimeter performance is based, and will continue to do so. We will continue to determine the factors that limit the performance of our prototypes and try to eliminate these factors, or least reduce their effects to insignificant proportions. Until this process has been completed, we will tend to ignore issues concerning the incorporation of this type of detector into a 4π experiment, and simulations in general.

So far, the dual-readout approach has been remarkably successful. It combines the advantages of compensating calorimetry with a reasonable amount of design flexibility. Since there is no limitation on the sampling fraction, the factors that limited the energy resolution of compensating calorimeters (SPACAL, ZEUS) to $\sim 30\%/\sqrt{E}$ can be eliminated, and the theoretical resolution limit of $\sim 15\%/\sqrt{E}$ seems to be within reach. Dual-readout detectors thus hold the promise of high-quality calorimetry for *all* types of particles, with an instrument that can be calibrated with electrons.

References

[1] Akchurin N *et al.* 1997, Nucl. Instr. and Meth. **A399**, 202.
[2] Wigmans R 2000, *Calorimetry, Energy Measurement in Particle Physics*, International Series of Monographs on Physics, Vol. 107, Oxford University Press (2000).
[3] Akchurin N *et al.* 2005, Nucl. Instr. and Meth. **A537**, 537.
[4] Akchurin N *et al.* 2008, Nucl. Instr. and Meth. **A584**, 304.
[5] Akchurin N *et al.* 2007, Nucl. Instr. and Meth. **A582**, 474.
[6] Gaudio G 2008, Contribution to these Proceedings.
[7] Voena C 2008, Contribution to these Proceedings.
[8] Akchurin N *et al.* 2008, Nucl. Instr. and Meth. **A584**, 273.
[9] Pinci D 2008, Contribution to these Proceedings.
[10] Drews G *et al.* 1990, Nucl. Instr. and Meth. **A290**, 335.
[11] Hauptman J 2008, Contribution to these Proceedings.
[12] Akchurin N *et al.* 2007, Nucl. Instr. and Meth. **A581**, 643.